

Supplementary Text

Given a single input and a single output, a linear transform relating the two can always be found (Press WHT, Saul A. Vetterling, William T. and Flannery, Brain P. 2007). With two sets of two inputs and two outputs, one can also always find a linear solution (proof to follow). For example, we might have both Gamma LFP power (input 1) and Alpha LFP power (input 2) from area V3 and from area PCC, and wish to find a set of linear transfer functions (TF1 and TF2) that relate these two inputs to the BOLD signals in each area (Output.a and Output.b). We can express this mathematically as follows:

$$\text{Input1.a} * \text{TF1} + \text{Input2.a} * \text{TF2} = \text{Output.a} \quad (1)$$

$$\text{Input1.b} * \text{TF1} + \text{Input2.b} * \text{TF2} = \text{Output.b} \quad (2)$$

Here each term is the time frequency representation of either LFP power (inputs) or the BOLD response (outputs). Multiplication in the frequency domain (“*”) is the same as convolution in the time domain (Press WHT, Saul A. Vetterling, William T. and Flannery, Brain P. 2007). Solving for the two transfer functions yields:

$$\text{TF1} = \frac{\text{Output.a} * \text{Input1.b} - \text{Output.b} * \text{Input1.a}}{\text{Input2.a} * \text{Input1.b} - \text{Input2.b} * \text{Input1.a}} \quad (3)$$

$$\text{TF2} = \frac{\text{Output.b} * \text{Input2.a} - \text{Output.a} * \text{Input2.b}}{\text{Input2.a} * \text{Input1.b} - \text{Input2.b} * \text{Input1.a}} \quad (4)$$

A finite solution exists so long as

$$\text{Input2.a} * \text{Input1.b} \neq \text{Input2.b} * \text{Input1.a}$$

$$\rightarrow \frac{\text{Input1.a}}{\text{Input1.b}} \neq \frac{\text{Input2.a}}{\text{Input2.b}} \quad (5)$$

In other words, if the ratio between Alpha and Gamma bands is not the same in V3 as it is in PCC, we are guaranteed to find a set of transfer functions that works for both V3 and PCC. More generally, we can replace Alpha and Gamma with any other pair of bands (for instance, Delta and Theta bands). Thus, by using two LFP bands, a mathematical solution can be found that will relate the LFP signals to the BOLD recorded in two different areas. However, given that this is guaranteed to work with any pair of LFP signals, it is doubtful that the solution will reflect anything of physiological interest.

Press WHT, Saul A. Vetterling, William T. and Flannery, Brain P. 2007.
Numerical Recipes: The Art of Scientific Computing Third Edition. Cambridge University Press.

Supplementary Figure S1



Figure S1. Examples of visual stimuli used in this study. The projector we used to deliver the stimuli blurred the visual stimuli, to an extent equivalent to applying a 2-pixel radius Gaussian filter to a 259 X194 pixel image. Two examples are shown to illustrate the effect of the blurring.

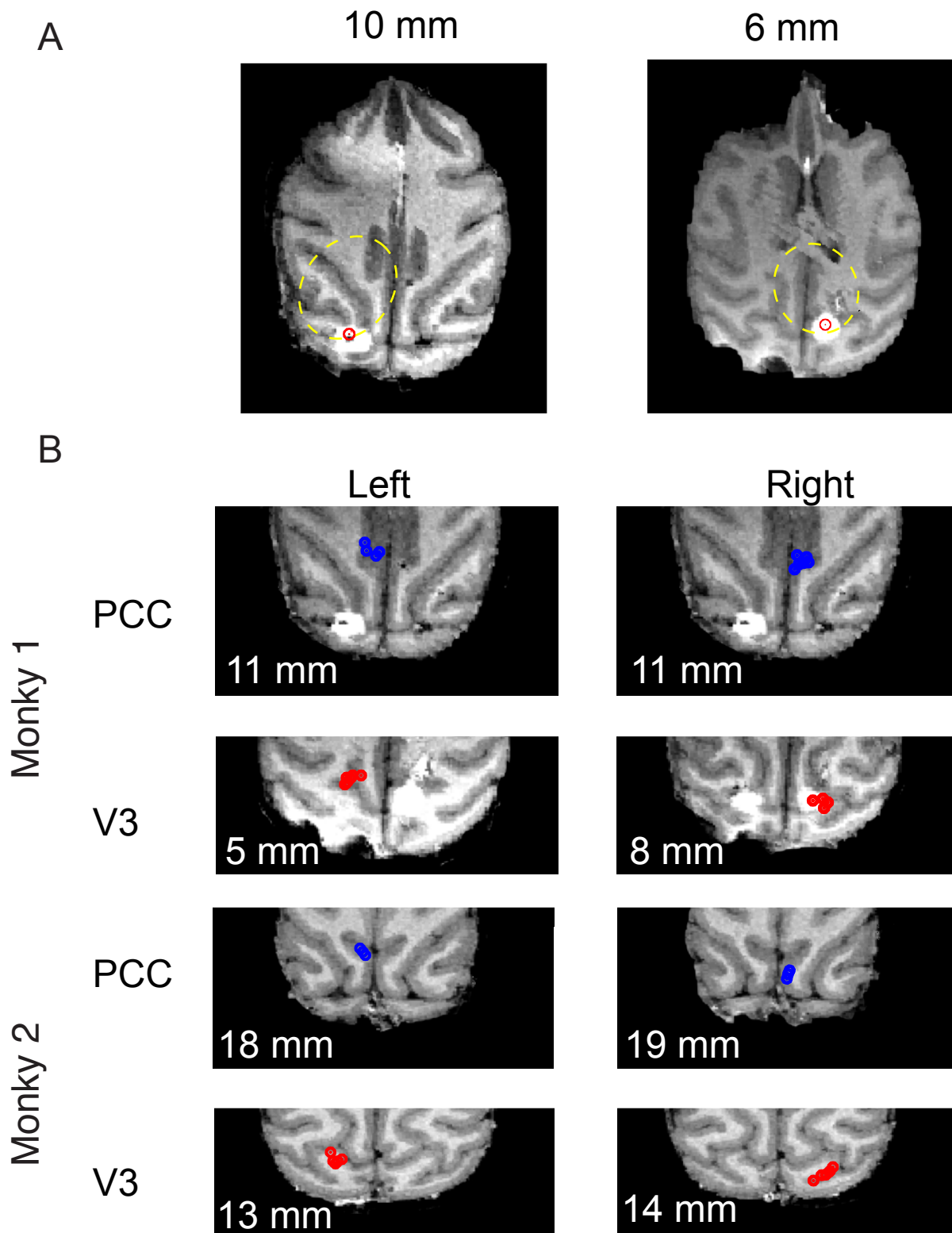


Figure S2. Recording sites confirmed by manganese injections. Manganese is MRI lucent and was used to calibrate our recording apparatus. A. MRI images showing injections into each hemisphere (white blobs) and the locations at which injections were aimed (red dots). The dots are aligned with the injections, confirming the accuracy of our maps. The dashed yellow ovals mark the boundaries of our recording chambers. B. Recording sites in the two monkeys (blue dots for PCC, and red dots for V3). Recordings into each hemisphere in each monkey are shown separately, often at a different slice depth. For example, the upper left panel shows PCC recordings into Monkey 1, left hemisphere. The slice depths indicate millimeters above the anterior commissure. The top of the brain is at 22 mm and 26 mm for Monkey 1 and Monkey 2, respectively.

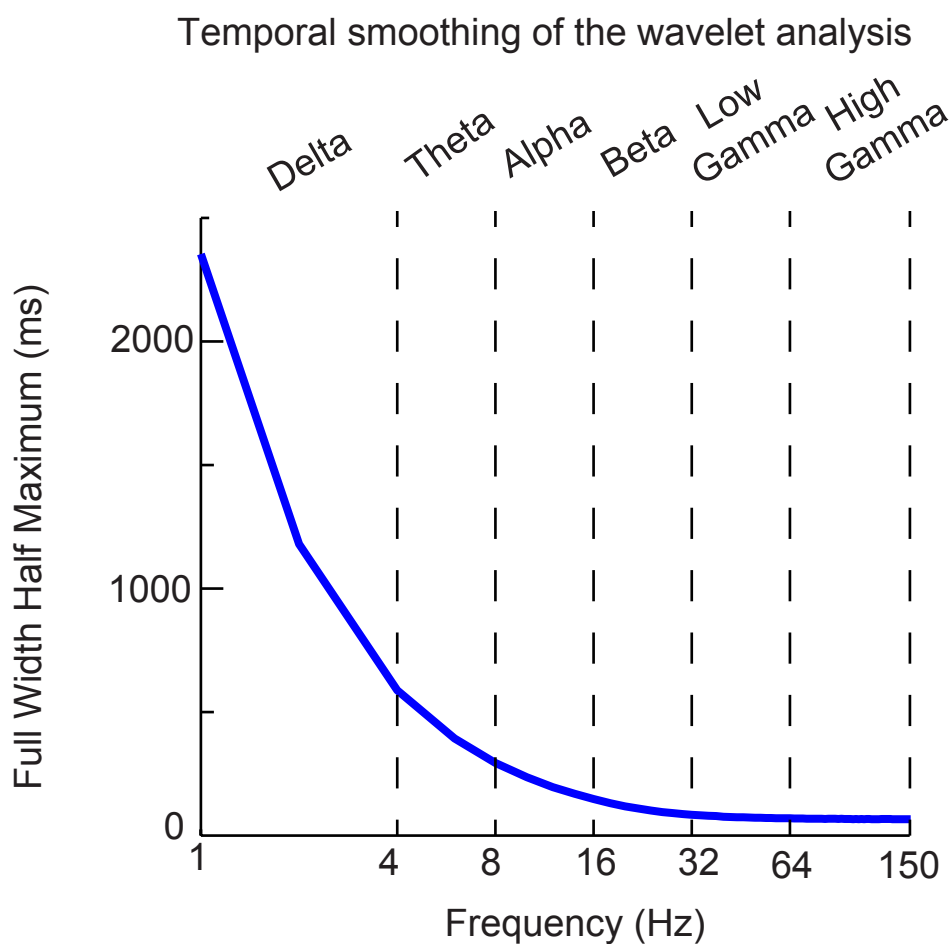


Figure S3. The temporal smoothing of the wavelet analysis. Power at specific frequency is estimated by convolving data with a complex Morlet wavelet. This method includes inherent low-pass temporal smoothing. The degree of smoothing is a function of frequency, and is similar to convolving the instantaneous power with a Gaussian. Here we show the full width of the equivalent Gaussian at half maximum height for each frequency. Notice that the degree of smoothing is greater for lower frequencies.

Supplementary Figure S4

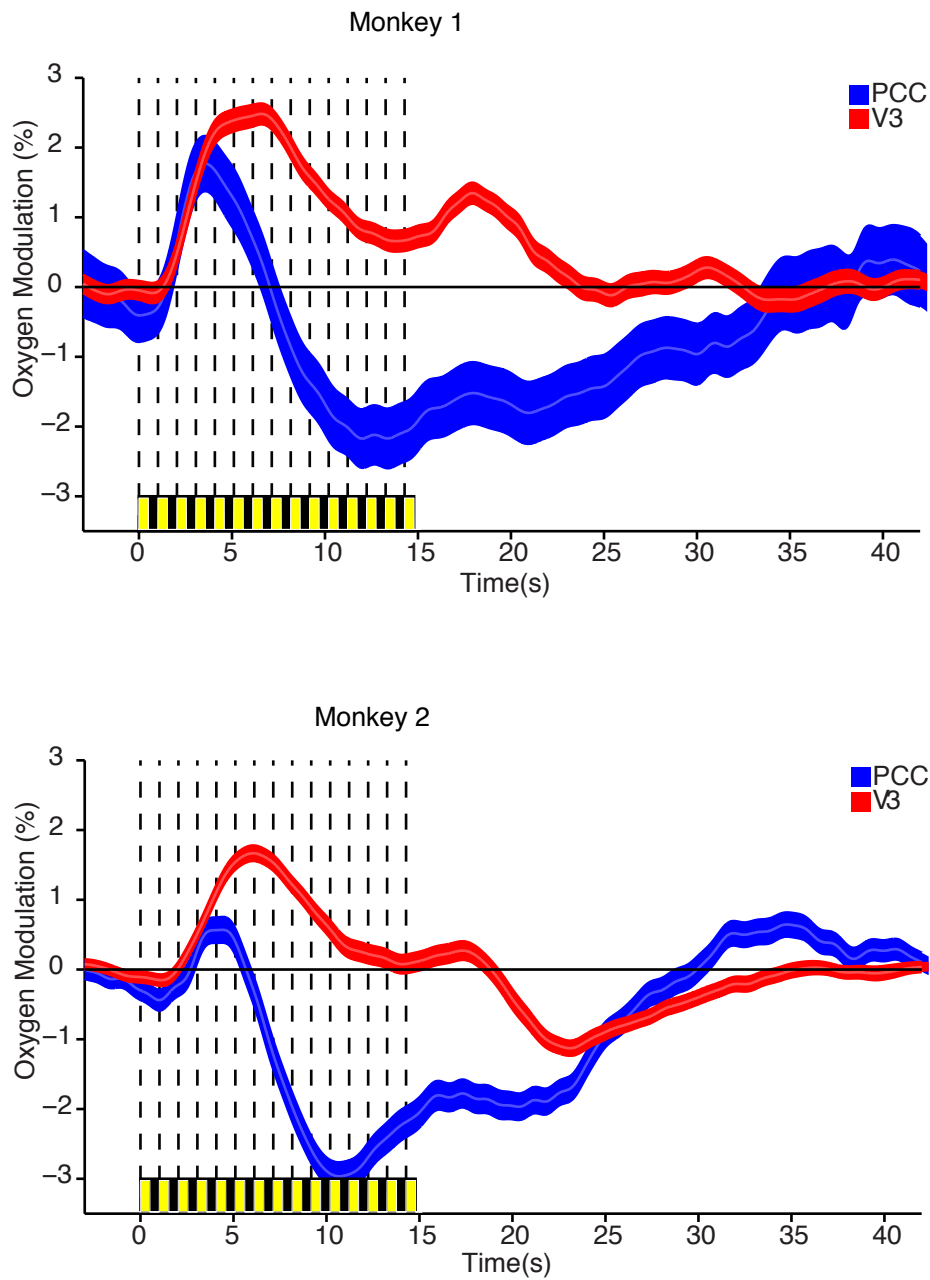


Figure S4. Percent oxygen modulation (mean \pm SEM) relative to the period 0-5 s before stimulus onset for both monkeys. In V3, oxygen level shows a transient response to the stimulus onset, followed by sustained activation. In PCC, oxygen level shows transient activation followed by sustained suppression. These are true for both monkeys.

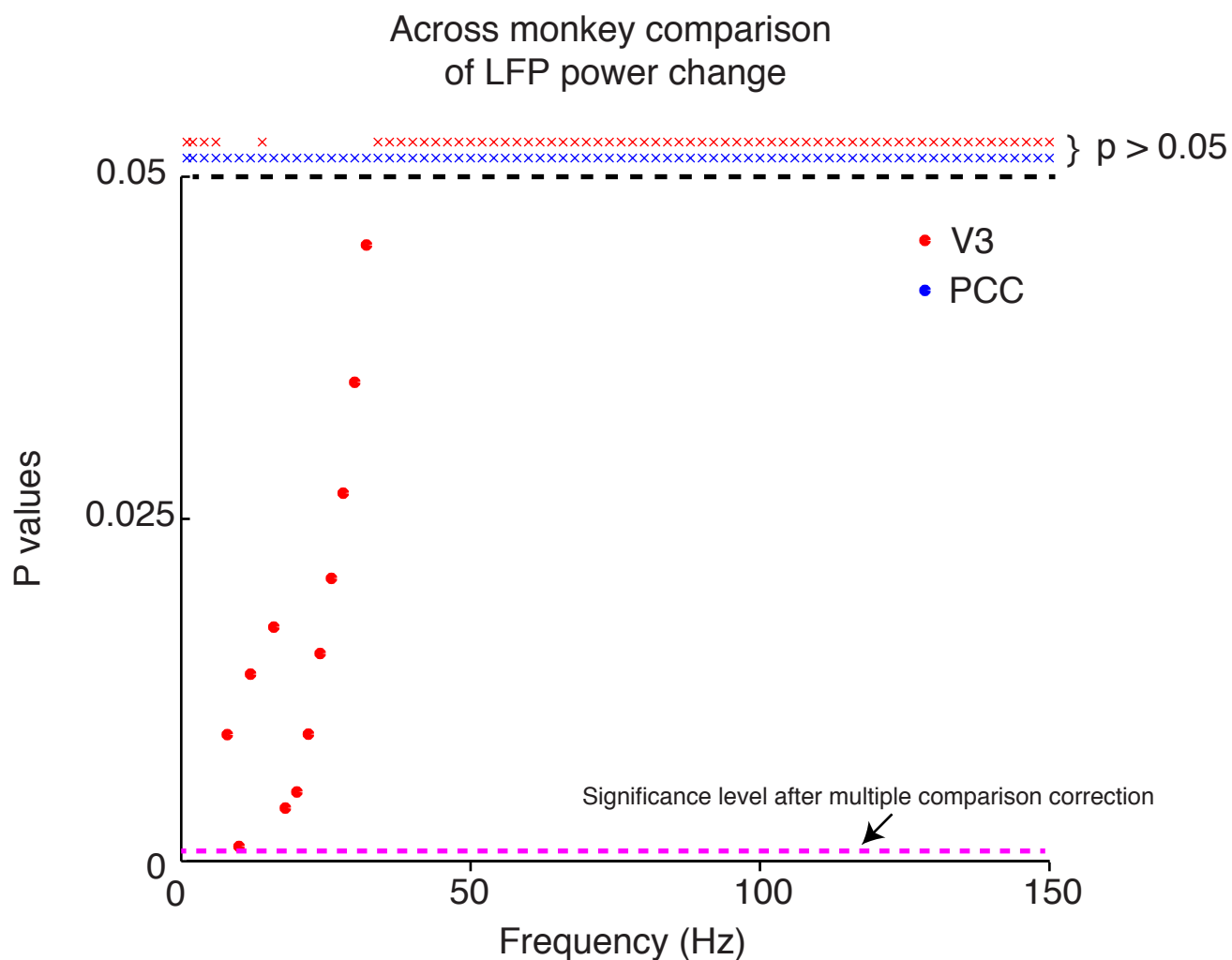


Figure S5. The p values (without multiple comparison correction) for the across monkey comparison of modulation in LFP power at each frequency. LFP power modulation is computed the same as in Figure 2B (5-15 s after the onset of visual stimulation relative to the subsequent 30 s of darkness). P values larger than 0.05 are shown as crosses. In PCC, there is no significant difference in power between the two monkeys at any frequency. In V3, there is no significant difference except at 8-32 Hz, where the LFP power modulation for Monkey 1 is less than that of Monkey 2. Even this difference is not significant if corrected for multiple comparisons (criterion level of $P = 0.05/76$, dashed magenta line).

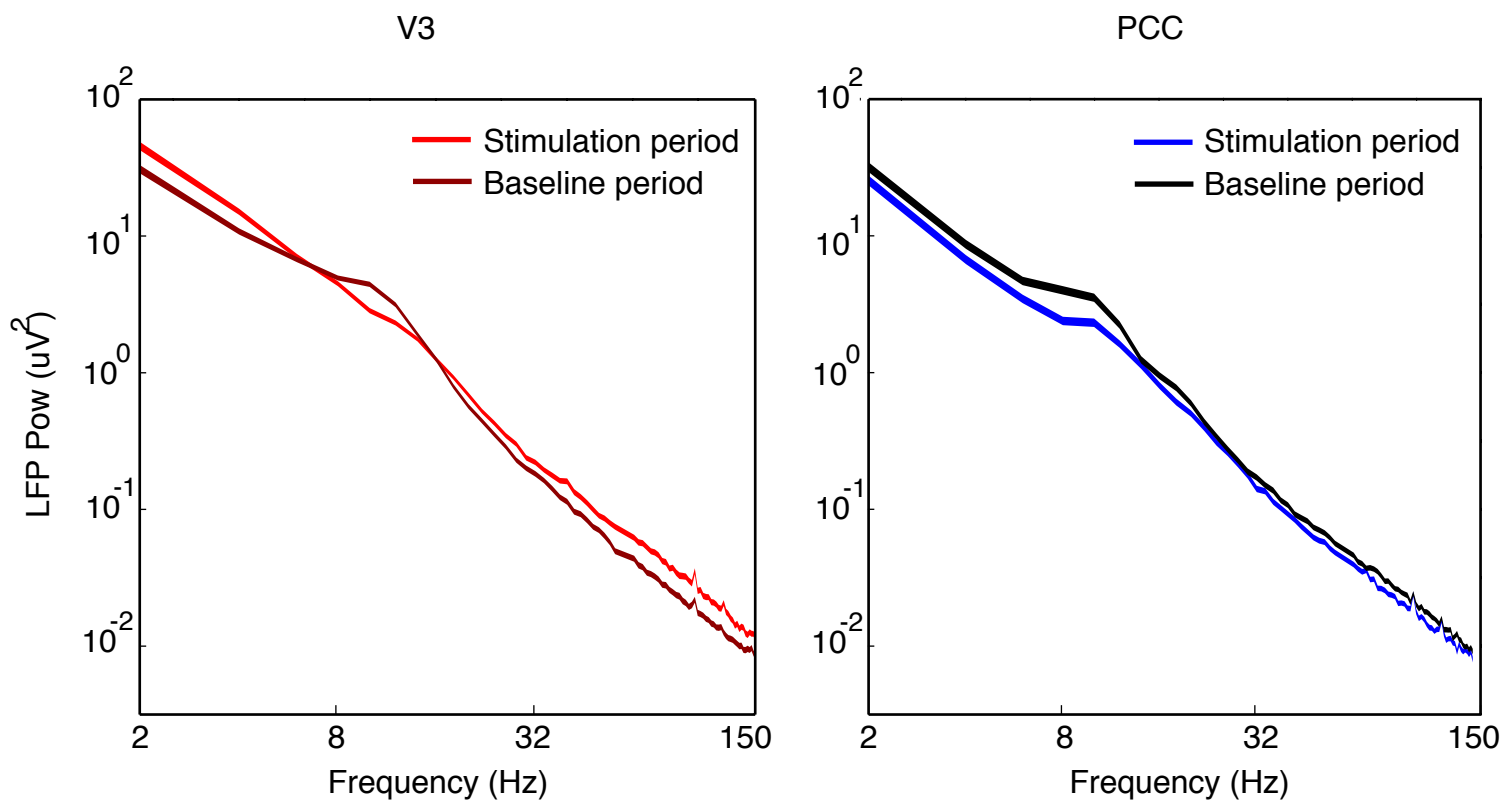


Figure S6. LFP power (mean \pm SEM) as a function of frequency (log) during stimulation for V3 and PCC for the visual stimulation period and the baseline period (0-5 s before stimulus onset). Overall, LFP power is inversely proportional to the frequency. In V3, LFP power increases during stimulation compared to the baseline, except for (6-16 Hz). In PCC, LFP power decreases during stimulation compared to the baseline.

Supplementary Figure S7

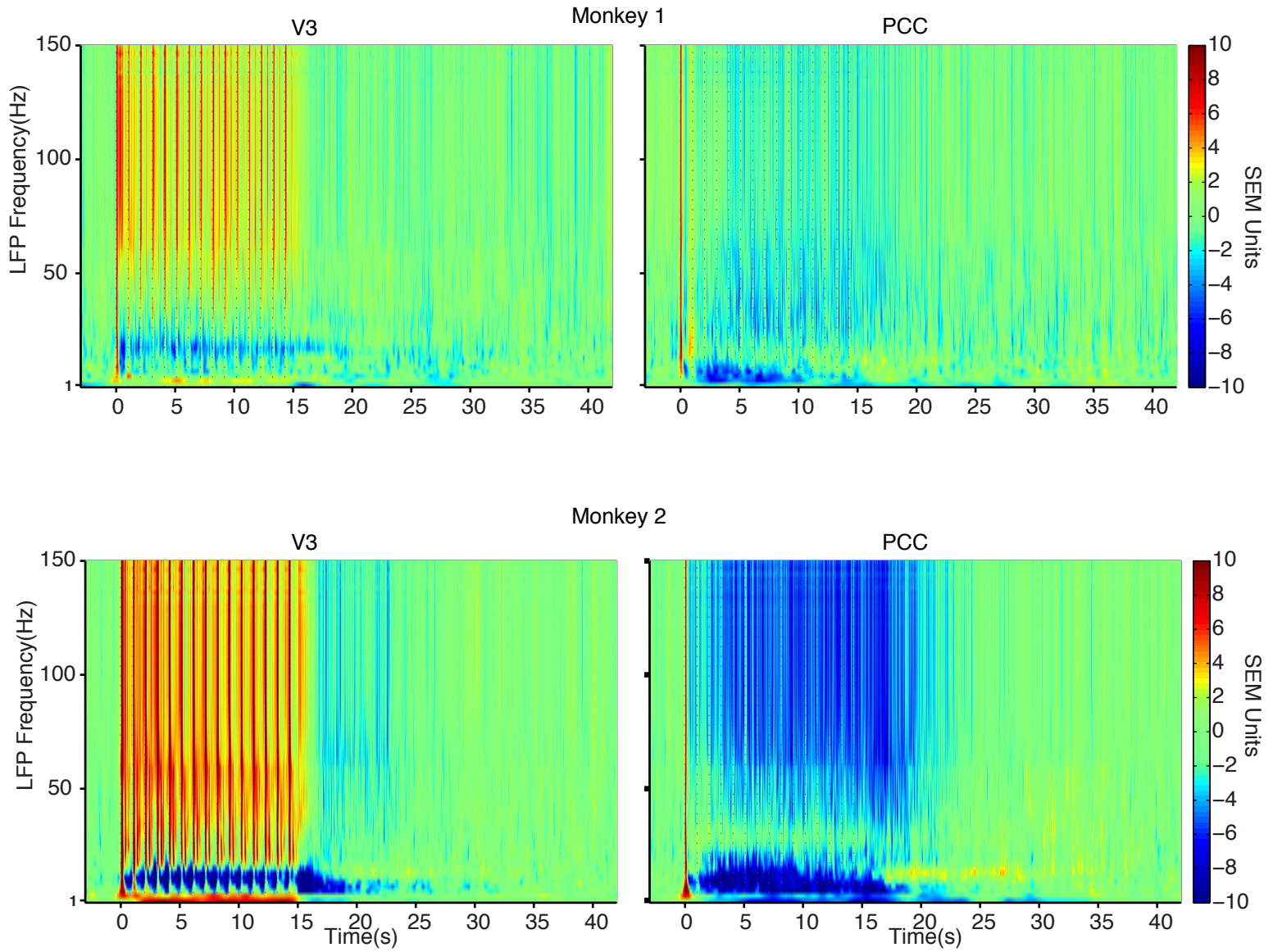


Figure S7. LFP power modulation relative to baseline (0-5 s before stimulus onset) in standard error units (SEM is estimated based on baseline activity) for both monkeys.

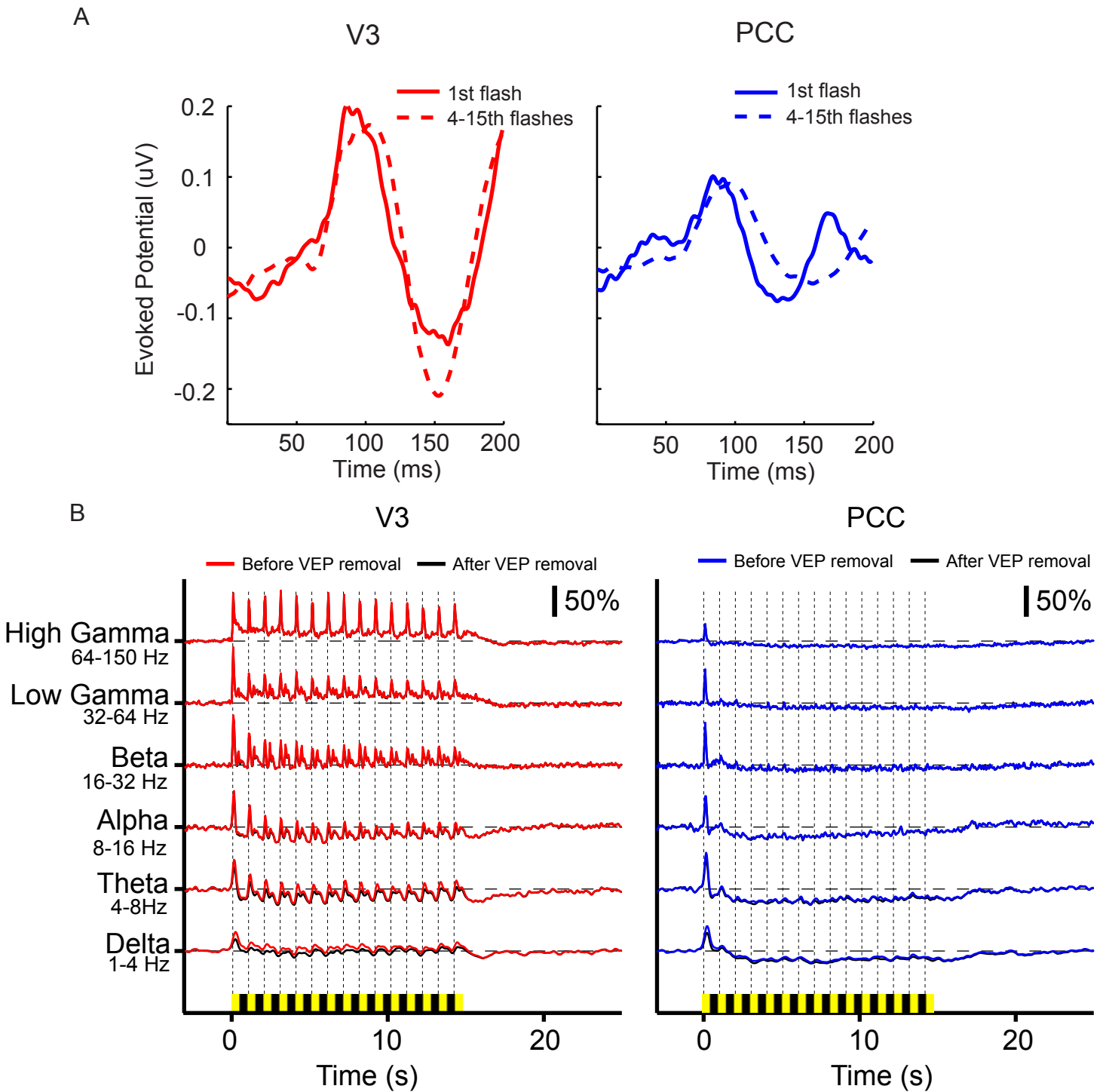


Figure S8. A. Visual stimulus evoked potential (VEP) for V3 and PCC. The positive component around 100 ms could correspond to the P100, and the negative component around 150 ms in V3 could correspond to the N140. VEPs associated with the stimulus onset (solid lines, first flash) are similar to those evoked by the later flashes (dashed lines, 4-15th flashes). This is different from oxygen responses, which show a prominent transient response to the stimulus onset and a sustained response (positive in V3 and negative in PCC) to later flashes. B. Percent modulation of LFP power for standard EEG bands before and after removing VEP. Removal of VEP slightly decreased LFP responses for both transient and sustained components, but the decrease is so small that the data before (colored) and after (black) VEP removal are almost indistinguishable.

Supplementary Figure S9

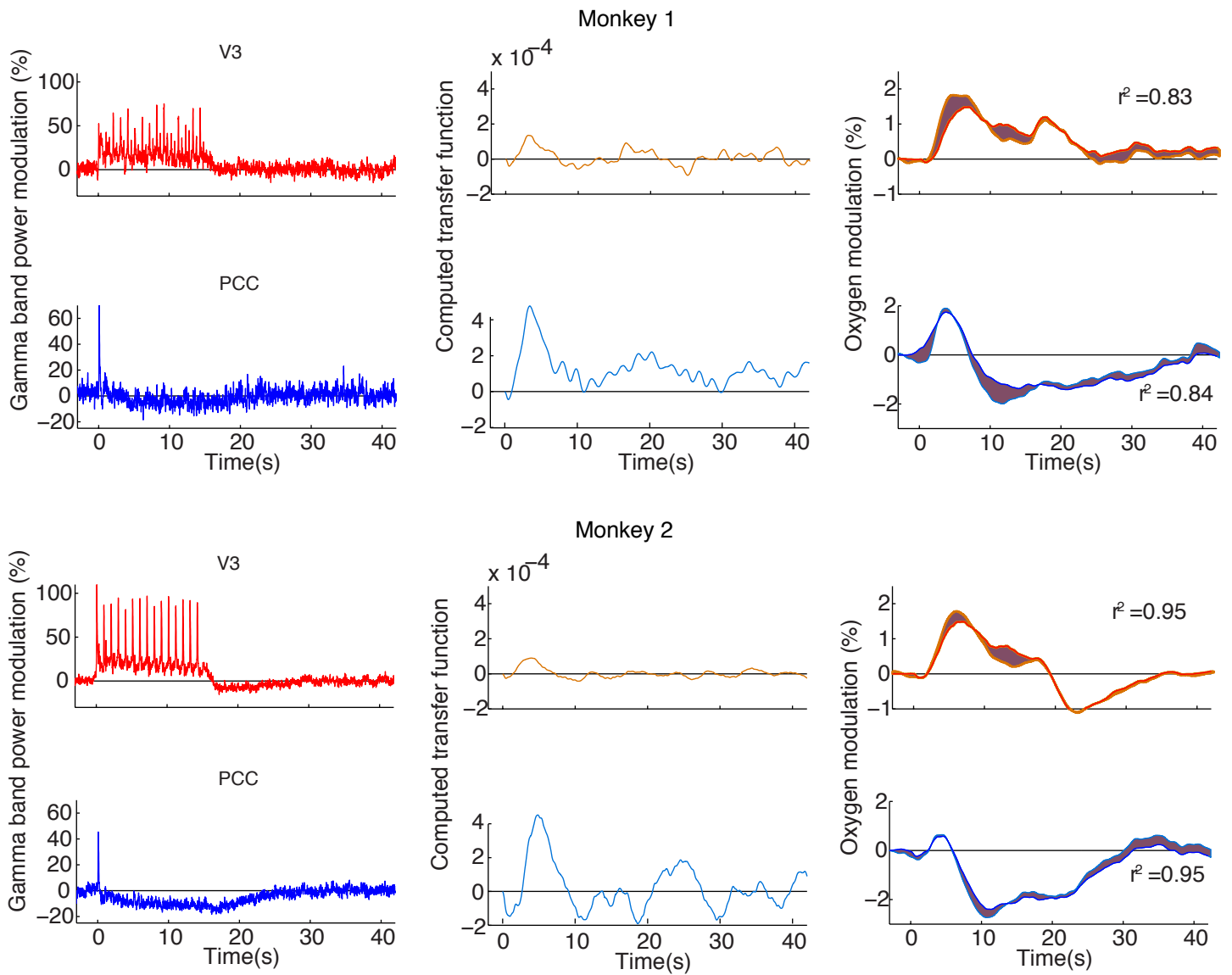


Figure S9. A computed transfer function (see text) does well in both areas but is smaller in V3 (orange in the second column) and contains an initial negativity only in PCC (cyan in the second column) for both monkeys.

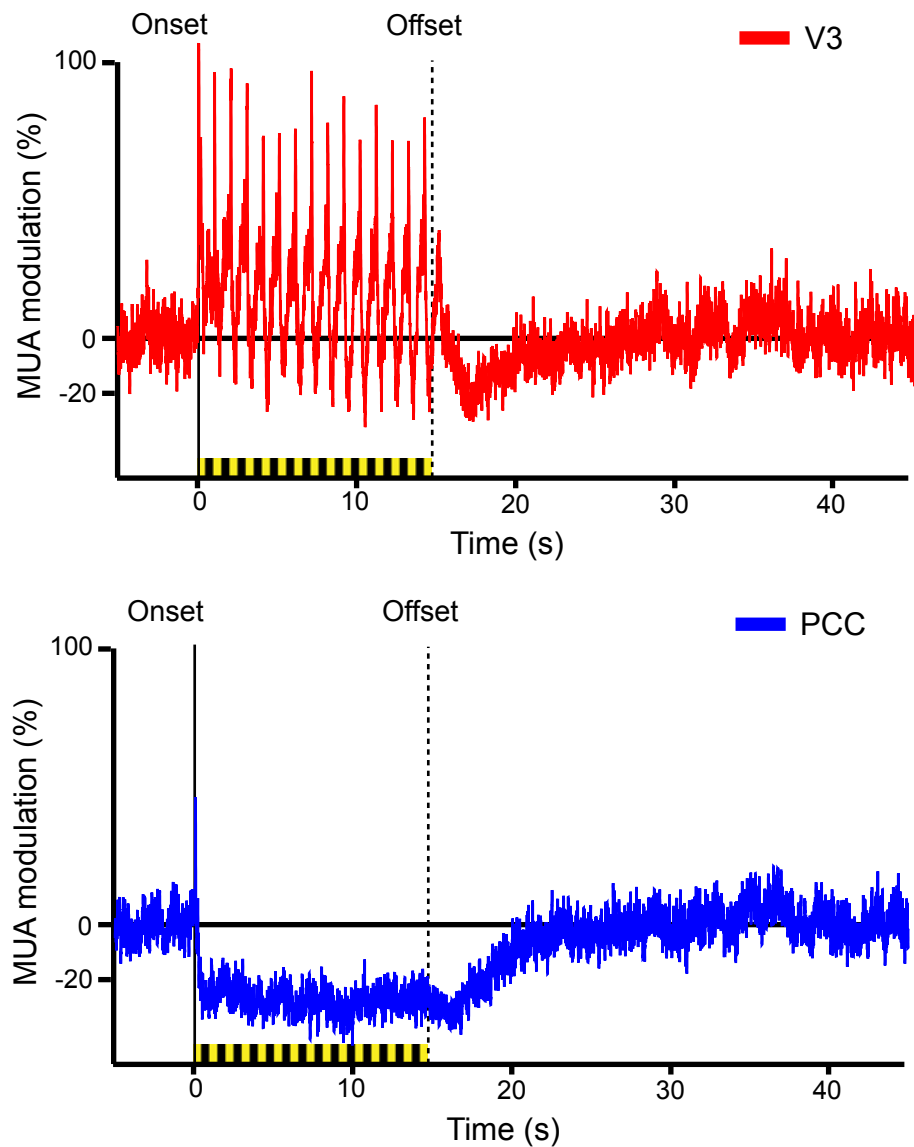


Figure S10. Percent multiple-unit activity (MUA) modulation relative to the period 0-5 s before stimulus onset. Yellow-black bars mark the 15 s, 1 Hz stroboscopic flashing stimulus. Electrophysiological signals were band-pass filtered (800Hz to 8kHz) and events exceeding 2.5 times the root mean square of the filtered signal were considered as MUA events. V3 shows complex phasic responses riding on top of a tonic increase in MUA activity relative to baseline. PCC shows smaller phasic responses at the onset of the first flash followed by a tonic decrease. Data from 397 trials in V3 and 398 in PCC from one monkey are included.